



Universiteit
Leiden

The Netherlands

Quantitative pharmacology approaches to inform treatment strategies against tuberculosis

Mehta, K.

Citation

Mehta, K. (2024, May 30). *Quantitative pharmacology approaches to inform treatment strategies against tuberculosis*. Retrieved from <https://hdl.handle.net/1887/3754903>

Version: Publisher's Version

License: [Licence agreement concerning inclusion of doctoral thesis in the Institutional Repository of the University of Leiden](#)

Downloaded from: <https://hdl.handle.net/1887/3754903>

Note: To cite this publication please use the final published version (if applicable).

Chapter 3

Pharmacogenetic variability and the probability of site of action target attainment during tuberculosis meningitis treatment: A physiologically based pharmacokinetic modeling and simulations study

Krina Mehta, Navaneeth Narayanan, Scott Heysell, Gregory P Bisson, Selvakumar Subbian, Natalia Kurepina, Barry N. Kreiswirth, Christopher Vinnard

Tuberculosis. Volume 137, December 2022, 102271.

Abstract

Objective and Methods: Our objective was to investigate the role of patient pharmacogenetic variability in determining site of action target attainment during tuberculous meningitis (TBM) treatment. Rifampin and isoniazid PBPK model that included *SLCO1B1* and NAT2 effects on exposures respectively were obtained from literature, modified, and validated using available cerebrospinal-fluid (CSF) concentrations. Population simulations of isoniazid and rifampin concentrations in brain interstitial fluid and probability of target attainment according to genotypes and *M. tuberculosis* MIC levels, under standard and intensified dosing, were conducted.

Results: The rifampin and isoniazid model predicted steady-state drug concentration within brain interstitial matched with the observed CSF concentrations. At MIC level of 0.25 mg/L, 57% and 23% of the patients with wild type and heterozygous *SLCO1B1* genotype respectively attained the target in CNS with rifampin standard dosing, improving to 98% and 91% respectively with 35 mg/kg dosing. At MIC level of 0.25 mg/L, 33% of fast acetylators attained the target in CNS with isoniazid standard dosing, improving to 90% with 7.5 mg/kg dosing.

Conclusion: In this study, the combined effects of pharmacogenetic and *M. tuberculosis* MIC variability were potent determinants of target attainment in CNS. The potential for genotype-guided dosing during TBM treatment should be further explored in prospective clinical studies.

Introduction

Central nervous system infection is the most severe manifestation of TB, with approximately one-half of affected patients suffering severe neurologic disability or death^{1,2}. In the absence of known or suspected drug-resistant disease, TB treatment guidelines recommend standard dosing of isoniazid and rifampin as part of the first-line regimen³. Clinical trials of intensified dosing of rifampin for tuberculosis meningitis (TBM) have yielded mixed results⁴⁻⁶, perhaps owing to differences in the dosing regimen of the intensified arm⁷. There still remains considerable uncertainty regarding the optimal initial treatment of TBM patients⁶.

For the treating clinician, limited information is available to guide the selection of a drug regimen for a TBM patient. The susceptibility of *M. tuberculosis* to a given anti-TB drug is typically established with phenotypic resistance testing at a “breakpoint” MIC, with a delay of several weeks after cultures are obtained⁸. While these breakpoint MIC values have been interrogated in the treatment of pulmonary TB⁹, the relationship between MIC breakpoint and clinical response in the treatment of TBM patients is less examined². Furthermore, there is an emerging understanding of the contribution of host genetics to the pharmacokinetic (PK) variability of both isoniazid and rifampin¹⁰. For isoniazid, this source of variability is primarily driven by the metabolizing enzyme responsible for isoniazid elimination, the N-acetyltransferase-2 (*NAT2*) gene¹¹. More recently, pharmacogenetic variability in the hepatic OATP1B1 uptake transporter gene (*SLCO1B1*) has been identified as a driver of rifampin PK variability, as individuals who possessed the variant allele demonstrated increased rifampin clearance compared to individuals with the homozygous wild-type gene^{12,13}.

For both isoniazid and rifampin, the pharmacodynamic effect is based on achieving PK exposure at the site of infection, defined by the area under the concentration-versus-time profile (AUC), that is sufficiently greater than the MIC of the infecting *M. tuberculosis* strain^{14,15}. Prior work has examined the impact of phenotypic drug resistance on the clinical outcomes of TBM, demonstrating that initial isoniazid and/or rifampin resistance is associated with death before treatment completion^{16,17}. We sought to extend this work by examining the likelihood of target attainment among TBM patients with putative drug-susceptible disease, as defined by MIC levels for isoniazid and rifampin below the CLSI breakpoint¹⁸. We hypothesized that sub-breakpoint MIC levels would correspond to unattainable targets among TBM patients with genotypes of *SLCO1B1* (for rifampin) or *NAT2* (for isoniazid) that correspond with lower systemic exposures.

Methods

Rifampin and isoniazid PBPK modeling with genotype effects of *SLCO1B1* and *NAT2*

A previously developed rifampin whole-body PBPK model was used as the base model¹⁹. The rifampin PBPK model included metabolism by enzyme arylacetamide deacetylase (AADAC), transport by organic anion-transporting polypeptide transporter (OATP1B1) and P-glycoprotein, along with the auto-induction of AADAC, OATP1B1, P-glycoprotein, and CYP3A4. Partition-coefficients from plasma to various tissues, including brain interstitial and intracellular compartments, were calculated based on Rodgers and Rowland method²⁰. The model included efflux transporter, P-glycoprotein, mediated passive transport through blood-brain barrier¹⁹. The model also included the effect of hepatic OATP1B1 (encoded by the gene *SLCO1B1*) on rifampin clearance (S3.1).

To quantify the effects of *SLCO1B1* pharmacogenetic variability on rifampin exposure, we first reviewed the available literature. A clinical study that included rifampin PK and *SLCO1B1* genotypes identified an association of *SLCO1B1* SNP c.463CC (rs11045819 wild type) or c.463CA (rs11045819 heterozygous) with plasma concentrations of rifampin in TB patients (n=72 pulmonary TB patients from Africa, North America, and Spain)¹³. We performed a comparison of this SNP with data collected in a prospective cohort study of 40 HIV/TB patients in Botswana and also identified an association between *SLCO1B1* rs11045819 and rifampin exposure¹². As such, only *SLCO1B1* rs11045819 heterozygous vs. wild type categories were selected for evaluations in our PBPK study. The rifampin PBPK model was calibrated using data from literature¹³ and the proportional effect of heterozygous category on the maximum transport rate ($V_{\max_{\text{OATP1B1}}}$) was estimated, with all other parameters kept unchanged from the original model. Next, we performed an external validation of the expanded rifampin PBPK model using the PK data from our Botswana study¹². Patients in the validation dataset were categorized into heterozygous or wild-type groups based on the rs11045819 SNP (S3.2). We validated this expanded rifampin PBPK model by overlaying the model-predicted rifampin concentrations, stratified by *SLCO1B1* genotype, with the observed PK data for both genotype categories. Once validated, we performed a sensitivity analysis of the expanded rifampin PBPK model. The sensitivity of the estimates in exposure metrics, including the AUC, C_{\max} , and half-life were examined, after introducing 10% variation in absorption and clearance parameters.

We utilized a previously published and validated whole-body PBPK model of isoniazid to simulate PK profiles in CNS compartments during TB treatment²¹. This model incorporated a complex metabolic network, including metabolism of isoniazid by N-acyl ethanolamine-hydrolyzing acid amidase (NAAA) and NAT2 enzymes, along with further metabolism and transport of the metabolites by various processes. Partition-coefficients from plasma to various tissues, including brain interstitial and intracellular compartments, were calculated based on PK-Sim standard method as incorporated in the software²².

Additional external validation of the rifampin and isoniazid for the purpose of our analysis was performed by comparing brain interstitial drug predictions against observed drug concentrations measured in cerebrospinal fluid (CSF) collected from TB patients who received various doses of rifampin and isoniazid^{5,23,24}. Upon completion of the external validations, the rifampin and isoniazid PBPK model, which included *SLCO1B1* and NAT2 covariate effects on drug exposures, respectively, were used for simulations and CNS target attainment evaluations.

Model codes

The isoniazid PBPK model was unchanged from the previously published version²¹ and is available at the GitHub repository <https://github.com/HenrikCordes/isoniazid-PBPK-model>. The updated rifampin PBPK model with *SLCO1B1* genotype effect is available at the GitHub repository <https://github.com/krinaj/RIF-INH-PBPK-Models>. Additional details about the isoniazid and rifampin PBPK model development, validation, and parameter estimates are available in literature^{19,20}.

Observed MIC distributions in *M. tuberculosis* isolates cultured from CSF in TBM patients

To understand the potential benefit of intensified dosing regimens at the population level, we directly measured the rifampin and isoniazid MIC levels in collection of *M. tuberculosis* isolates that had been obtained from TBM patients in the U.S. state of New Jersey over a 12-year period. In support of statewide molecular epidemiology efforts, the Kreiswirth laboratory routinely performs DNA fingerprinting on all *M. tuberculosis* isolates across the state of New Jersey, recording the anatomic site of culture for each of isolate in the collection²⁵. Among those *M. tuberculosis* isolates that had been cultured from CSF and previously determined to be susceptible to both rifampin and isoniazid (n=34), we determined the MIC for rifampin and isoniazid by agar diffusion²⁶.

Target attainment under standard and intensified dosing schemes of isoniazid and rifampin

Isoniazid and rifampin concentrations in venous blood plasma and brain interstitial fluids were simulated using PBPK models. The simulated population contained 1,000 virtual adult TBM patients with body weight sampled from prior distribution of body weight from TB patients¹². Additionally, other physiological and anatomical parameters were varied as described previously to generate the virtual population²¹. Next, we performed separate simulations ($n=1,000$) for each *NAT2* (slow, intermediate, and fast acetylators) and *SLCO1B1* (wild-type and heterozygous) genotype²⁷. Under each dosing scheme (standard or intensified), the isoniazid or rifampin AUC_{0-24} following the 10th dose was calculated for brain interstitial fluid compartment.

Next, we calculated the AUC_{0-24}/MIC ratio corresponding to each MIC value for the infecting *M. tuberculosis* strain. Since all MIC values were falling below the breakpoint that defines drug susceptibility or resistance, we also calculated target attainment at higher MIC referring to drug-resistant strains²³. For each MIC value, we estimated probabilities of target attainment in brain interstitial fluid for both drugs, under standard and intensified dosing strategies. For rifampin, the target was defined as an AUC_{0-24}/MIC ratio of 30, corresponding to a 1 \log_{10} CFU/mL decrease in *M. tuberculosis* bacterial load²⁸. Based on the same criteria, the isoniazid target was defined as an AUC_{0-24}/MIC ratio of 43.5¹⁴. We selected intensified dosing strategies based on published clinical trial experiences^{23,24,29}. Additionally, based on observed MIC distributions at the population level, cumulative fraction of response under standard and intensified dosing strategies was estimated by sampling from observed distribution of MIC values in CSF of TB patients.

Software

Physiologically-based PK modeling and simulation was performed in PK-Sim[®] and Mobi[®] (Open Systems Pharmacology Suite, v8.0, www.open-systems-pharmacology.org). Statistical analysis and plots were generated in R (R for Windows, v4.1, <https://www.r-project.org/>) using RStudio (RStudio, v1-554, www.rstudio.com/).

Results

Extension of rifampin PBPK model with *SLCO1B1* genotype effects

The rifampin and isoniazid PBPK models included all major contributing factors affecting systemic and CNS exposures, including, protein binding, active and passive transports into various tissues, and relevant metabolism networks. As such, these models were selected for the purpose of our analysis. The updated rifampin PBPK model described observed plasma concentrations for both patients with both wild type and heterozygous *SLCO1B1* genotypes (**Figure 3.1a**). The model suggested a 3% proportional increase in OATP1B1 V_{max} among heterozygous genotype patients, compared to wild-type genotype patients (OATP1B1 V_{max} WT = 0.37 $\mu\text{mol/L/min}$ vs. OATP1B1 V_{max} WT = 0.39 $\mu\text{mol/L/min}$)¹³. All other parameters, other than OATP1B1 V_{max} , remained unchanged from the literature-based model¹⁹. In an external validation exercise, the simulated plasma concentration-time profile agreed well with observed rifampin PK data ($R^2=0.96$ and 0.93 , respectively, $p\text{-value}<0.0001$) for both *SLCO1B1* genotypes (**Figure 3.1b**). With a 10% change in parameter estimates, the sensitivity for key rifampin PK parameters was low (between -1 and 1), which further supported the reliability of the rifampin expanded PBPK model.

Model-predicted isoniazid and rifampin exposures in CNS, stratified by genotype

The rifampin and isoniazid PBPK models predicted steady-state drug concentration within brain interstitial compartment matched well with observed CSF drug concentrations (**Figure 3.2, Figure 3.4**). With the standard rifampin dose of 10 mg/kg orally once daily, the mean AUC_{0-24} ratio for brain interstitial fluid: plasma was predicted to be approximately 0.36 and 0.24 for wild-type and heterozygous groups, respectively. For the standard isoniazid dose (5 mg/kg), the mean AUC_{0-24} ratio for brain interstitial fluid: plasma was predicted to be approximately 0.76 for fast acetylators and 0.78 for both intermediate and slow acetylators.

Figure 3.1 Development and validation of an expanded rifampin PBPK model to include SLCO1B1 genotype. (A) Development of the model to include SLCO1B1 covariate effects (n=72 patients from Weiner et al, 2010¹³). (B) Validation of the expanded rifampin PBPK model (n=40 patients from Vinnard et al, 2017¹²). Rifampin PBPK model described plasma concentrations time profiles for both SLCO1B1 wild type and heterozygous groups well. Black points with error bars represent mean and SD of observed data, black points represent individual concentrations data, black line represent median of predicted, and grey shading represent 95% confidence interval of the predictions.

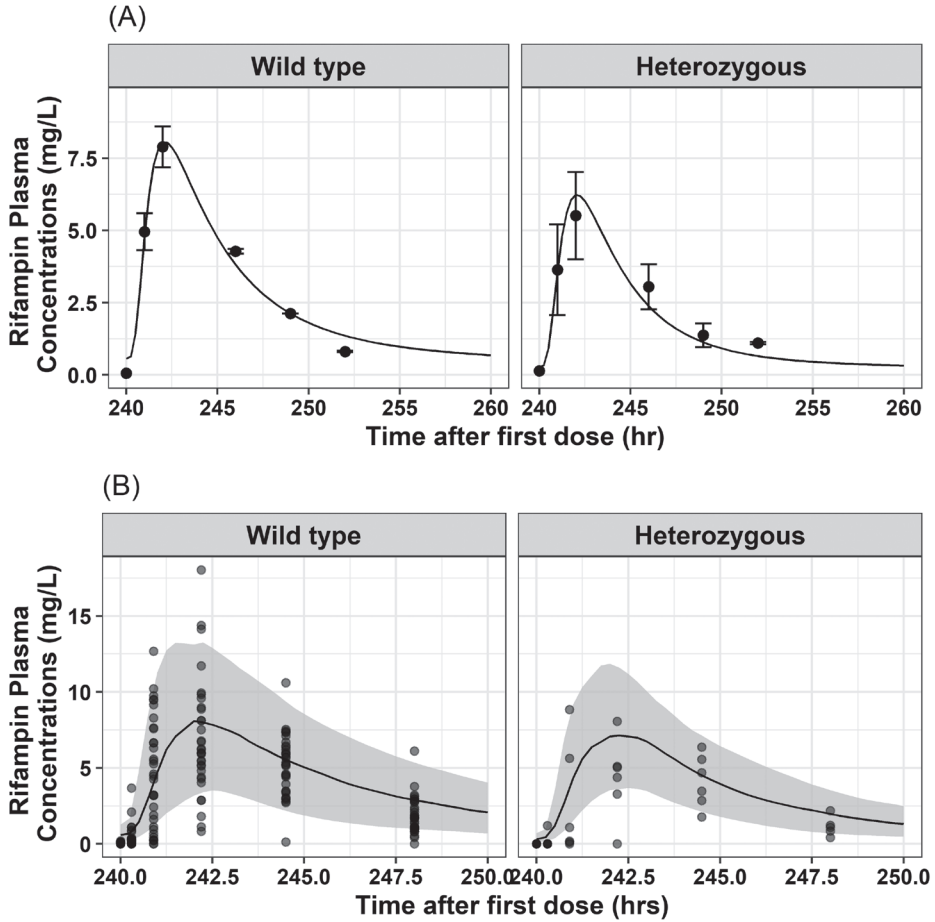


Figure 3.2 Validation of the rifampin and isoniazid PBPK models for predictions of drug exposures in the CSF. The PBPK models predicted rifampin and isoniazid steady-state concentrations in brain interstitial compartment matched well with the observed concentrations data from CSF of TB patients^{23,24}.

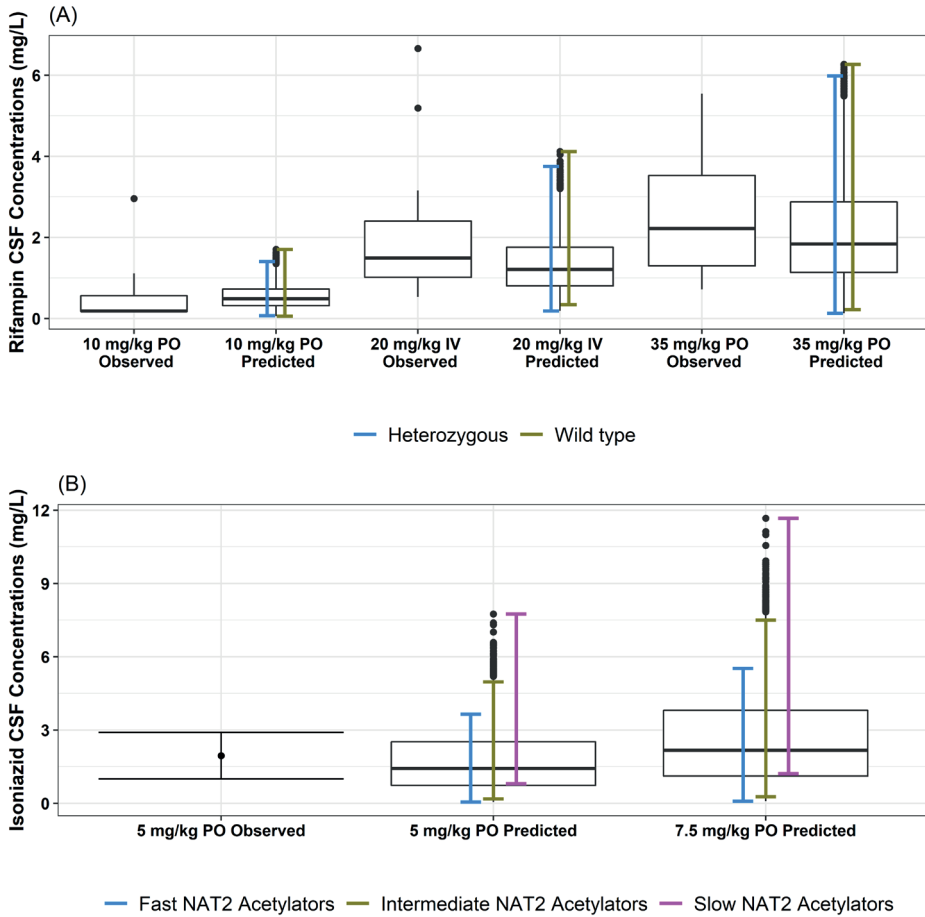
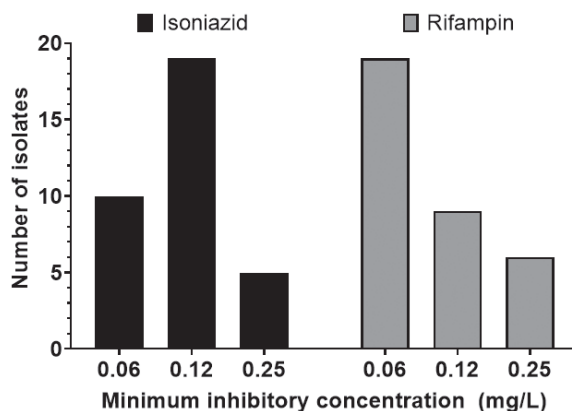


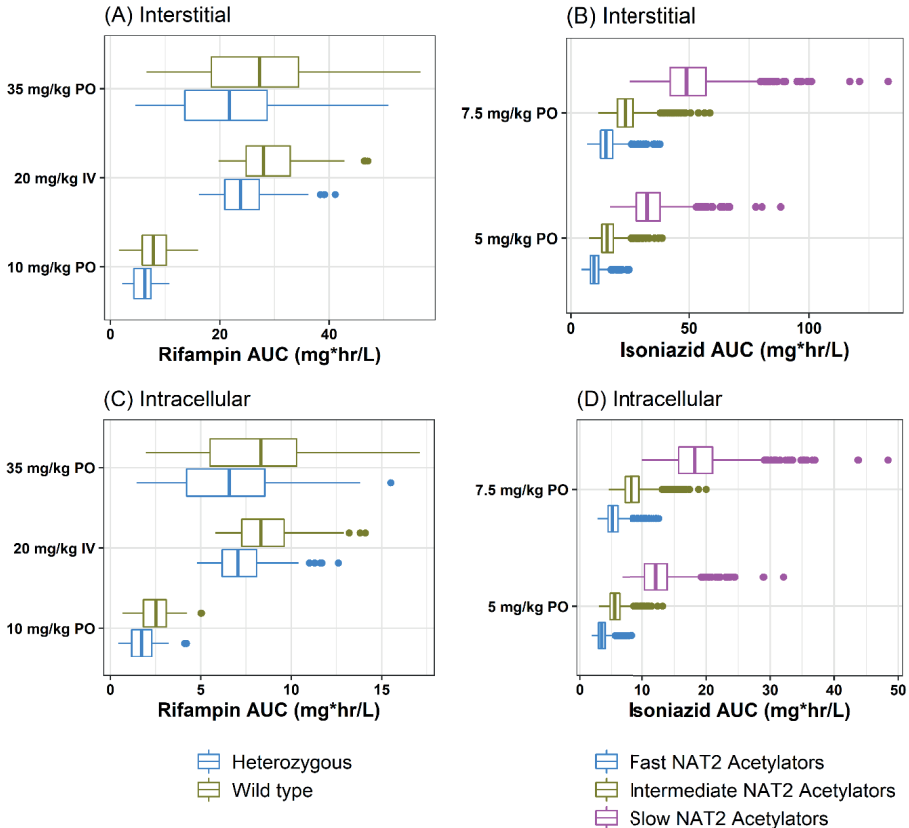
Figure 3.3 Distribution of minimum inhibitory concentration levels of isoniazid and rifampin among *M. tuberculosis* isolates that were cultured from CSF in New Jersey over a 12-year period.



Probability of target attainment in CNS under standard and intensified treatments

Distribution of MIC levels for rifampin and isoniazid in a collection of *M. tuberculosis* isolates that had been cultured from the CSF of patients is presented in **Figure 3.3**. With standard and intensified rifampin dosing, the probabilities of successful rifampin target attainment in brain interstitial fluid are shown in **Figure 3.5A**. At rifampin MIC level of 0.125 mg/L, 92% of patients with wild-type *SLCO1B1* genotype attained the rifampin target in brain interstitial fluid, compared with 86% of the patients with heterozygous *SLCO1B1* genotype. At a rifampin MIC level of 1 mg/L, none of the patients with either *SLCO1B1* genotype were predicted to achieve rifampin target in brain interstitial fluid. With intensified rifampin dosing of 35 mg/kg and MIC level of 1 mg/L, 42% and 21% of patients with wild-type and heterozygous *SLCO1B1* genotype, respectively, attained the rifampin target in brain interstitial fluid. With standard and intensified rifampin dosing, the probabilities of successful isoniazid target attainment in brain interstitial fluid are shown in **Figure 3.5B**. At an isoniazid MIC level that is less than or equal to 0.125 mg/L, nearly all TBM patients regardless of *NAT2* genotypes attained the target in brain interstitial fluid at the standard dosing. At an isoniazid MIC level of 1 mg/L, none of the fast or intermediate acetylators and only 12% of slow acetylator patients attained the target in brain interstitial fluid at the standard dosing. At the same MIC, intensified dosing predicted to provide target attainment in none of the fast acetylators, 2% of intermediate acetylators, and 68% of slow acetylators.

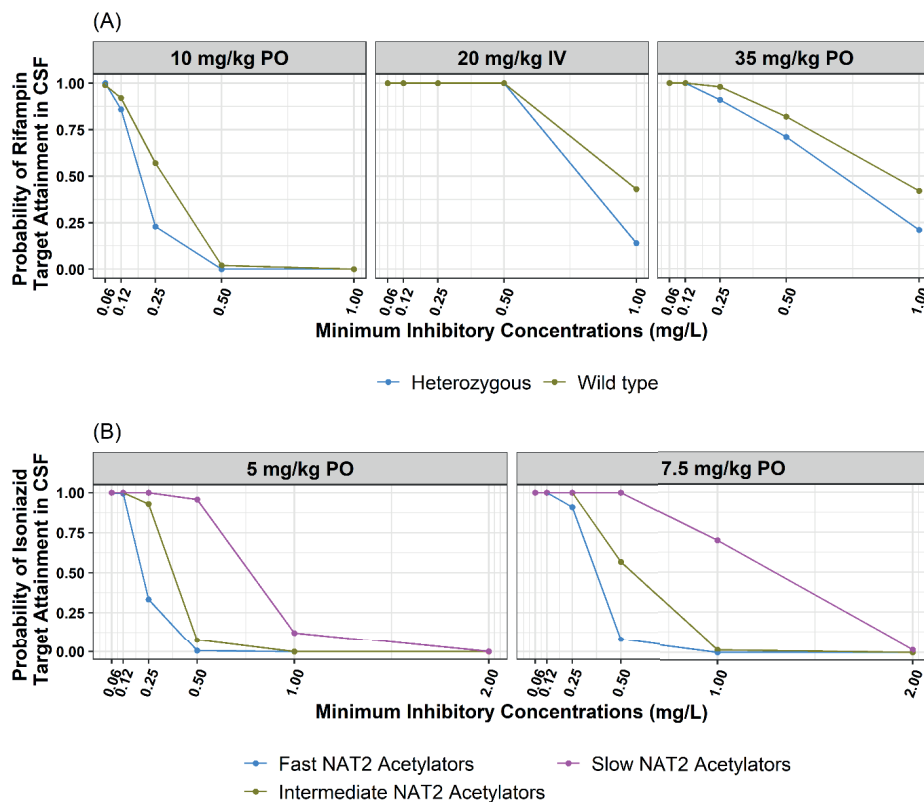
Figure 3.4 Predicted steady state rifampin and isoniazid AUC₀₋₂₄ (mg·hr/L) in the CNS compartments stratified by dosing regimen and genotype. (A) rifampin brain interstitial, (B) isoniazid brain interstitial, (C) rifampin brain intracellular, (D) rifampin brain interstitial. All dosing regimens were administered once daily.



3

Based on observed MIC distributions at the population level (**Figure 3.3**), cumulative fraction of response under standard and intensified dosing strategies was estimated by sampling MIC values from observed distribution of MIC values in CSF of TB patients to calculate target attainment probabilities. For the drug-susceptible strains, there was 86% and 99% overall probability of PD target attainment in brain interstitial fluid with standard dosing and intensified dosing of rifampin, respectively. Similarly, for the drug-susceptible strains, there was a 92% and 99% overall probability of target attainment in brain interstitial fluid with standard dosing and intensified dosing of isoniazid, respectively.

Figure 3.5 Target attainment probabilities in brain interstitial compartment under standard and intensified dosing regimens for rifampin and isoniazid stratified by *SLC01B1* and *NAT2* genotypes, respectively. All dosing regimen assumed once daily therapy.



Discussion

Our objective was to evaluate the probability of target attainment in the CNS during TBM treatment with a first-line regimen that includes isoniazid and rifampin. We used a PBPK modeling approach to incorporate two independent sources of variability: host pharmacogenetics and pathogen MIC levels. Using this approach, we tested the hypothesis that sub-breakpoint MIC levels for isoniazid and rifampin would correspond to essentially unattainable targets among patients with fast elimination genotypes. While our findings support this hypothesis, they also demonstrate that the clinical benefit of intensified dosing regimens are concentrated at certain MIC levels for the infecting *M. tuberculosis* strain.

Adequate PK exposures of anti-TB drugs in the CNS are crucial for treatment success for TBM patients³⁰. Current bioanalytical sampling methods do not allow measurements of drug exposure from various CNS sites of TB lesions, such as brain intracellular tuberculomas, and CSF drug concentrations may be used as a summary measure of CNS drug exposure³¹. The whole-body PBPK model that was used in this analysis includes blood cells, plasma, interstitial space, and tissue space for each organ/compartment; drug partitioning into these spaces is based on physicochemical parameters of the drug and physiological parameters of the species. Furthermore, the rifampin PBPK model also includes P-glycoprotein transporter effects at the blood-brain barrier¹⁹. As such, our PBPK model-based approach in this analysis is useful to predict anti-TB drug target attainment at CNS sites of action in TBM patients, and advances prior understandings based on CSF concentration-time profiles³²⁻³⁴.

In clinical trials of pulmonary TB patients, intensified dosing of rifampin (up to 50 mg/kg oral) led to fast sterilization activity increasing toxicity^{23,29,35}. In TBM patient populations, clinical trials of intensified rifampin dosing have shown mixed results. Rifampin doses up to 15 mg/kg did not show improved survival in a study conducted in Vietnamese patients (n=817)⁴. In contrast, a clinical trial of intensified rifampin dosing among Indonesian TBM patients (n=122) led to improvements in mortality without an increased rate of adverse events, with dose increases up to 30 mg/kg⁵. A model-based meta-analysis has found that even doses beyond 30 mg/kg may be expected to improve clinical response³³. Our work also suggests that unmeasured MIC variability may be a major driver of clinical response, with an additional contribution of *SLCO1B1* pharmacogenetic variability in some populations. Importantly, the MIC variability in the current study was entirely sub-breakpoint, meaning that these isolates would be classified as drug-susceptible by the clinical laboratory. With the PBPK model-based simulations, we were able to demonstrate that standard dosing would achieve markedly low probabilities for target attainment for drug-resistant strains by setting MIC to higher values. We propose that future prospective clinical trials of TBM treatment regimens prioritize the capacity for secondary analyses based on these additional sources of variability.

As patient genotyping methods advance to reach a greater number of bedsides in geographic areas with a high burden of TB disease, the potential tradeoffs between personalized medicine and standardized treatment regimens will require greater consideration, regarding incremental benefits and resource utilization. Much attention has been focused on the support of clinical decision-making provided

by DNA sequencing of *M. tuberculosis* strains, for example to identify mutants likely to confer phenotypic drug resistance³⁶. Yet parallel efforts are underway to identify the patient's genotypic determinants of TB treatment response, including the use of the *LTA4H* genotype to select patients for adjunctive corticosteroid treatment³⁷, currently studied in a prospective clinical trial³⁸. Our findings suggest that these patient genotyping efforts should be expanded to evaluate prospectively the impact of SNPs related to *NAT2* and/or *SLCO1B1* activity during TBM treatment. This information could be combined with *M. tuberculosis* mutational analysis to identify those patients most likely to benefit from intensified drug therapy, and perhaps to guide further the selection of the intensified dose in the regimen.

A key finding of the current work was the difference in drug exposures between brain interstitial fluid and brain intracellular. According to one model of TBM pathogenesis, the early bloodstream dissemination of *M. tuberculosis* may lead to foci of infection established in the meninges and brain parenchyma, following a vascular distribution³⁹. As these tubercles enlarge, there is potential for rupture into the sub-arachnoid space, leading to the signs and symptoms of meningitis, most commonly in a basilar distribution⁴⁰. Yet the tubercles themselves are found in the brain or meningeal tissue, and enlargement without rupture leads to the formation of tuberculomas, which may become clinically apparent as space-occupying lesions. Delayed sterilization of deep CNS anatomic sites during TB treatment, as a consequence of sub-optimal PK exposures, could contribute to the observed risk of paradoxical reaction during TBM treatment⁴¹. The current PBPK model calculated brain interstitial to intracellular partition coefficients based on standard PBPK modeling methods⁴². As such, the model may not contain all relevant mechanistic details pertaining drug penetration in the brain intracellular compartment. Although further work may be needed to implement all relevant mechanisms of brain intracellular penetration for anti-tuberculosis drugs, our relatively simple adaptation of whole-body PBPK model provide a quantitative estimate of the PK exposures of isoniazid and rifampin in brain intracellular, relative to brain interstitial fluid.

Our study had several notable limitations. The pharmacogenetic association of *SLCO1B1* variability with lower rifampin exposures was based on analysis from two independent clinical studies, and we recognize that heterozygous alleles at additional loci likely relate to rifampin PK variability⁴³. In pharmacogenetic studies that were reported subsequent to the work used in our PBPK model development and validation, the rs11045819 allele was found to be rare in certain populations⁴⁴. Linkage disequilibrium analyses, both between- and within- populations, will be

essential to improve understanding of the SNPs tags that correspond to gene function⁴⁵. For simplicity, we assigned the drug dose (mg) based on body weight (kg), rather than using dosing bands that allow for fixed-dose combination, and the additional impact of weight-based dosing bands would be of interest in a future study⁴⁶. Furthermore, recent clinical trials have also studied even higher rifampin doses than we selected for simulation purposes, up to 50 mg/kg⁴⁷. Strengths of our approach included the utilization of previously validated PBPK models for each drug, the formal validation of the *SLCO1B1* genotype as a novel covariate effect in the rifampin PBPK model, and the additional measurements of MIC distributions for isoniazid and rifampin among *M. tuberculosis* isolates cultured from TBM patients.

In summary, our PBPK-based approach demonstrated that the likelihood of target attainment during TBM treatment is jointly influenced by host pharmacogenetics and pathogen MIC variability. Within a PK-PD framework, the combination of these factors also identifies those patients most likely to benefit from intensified drug therapy. We propose that prospective clinical trials of TBM therapies should routinely capture these determinants of clinical response.

References

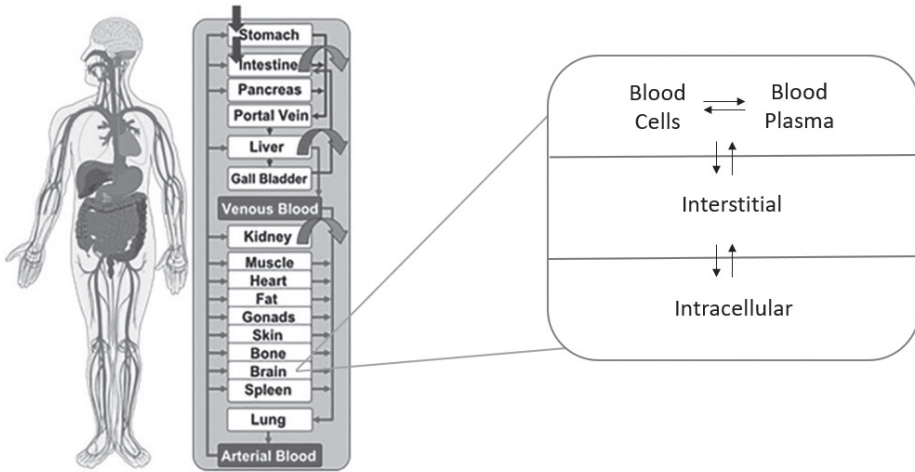
1. Seddon JA, Wilkinson R, van Crevel R, Figaji A, Thwaites GE, Aarnoutse RE, et al. Knowledge gaps and research priorities in tuberculous meningitis. *Wellcome Open Res.* 2019;4:1–18.
2. Mezocho A, Thakur K, Vinnard C. Tuberculous Meningitis in Children and Adults: New Insights for an Ancient Foe. *Curr Neurol Neurosci Rep.* 2017;17(11).
3. Nahid P, Dorman SE, Alipanah N, Barry PM, Brozek JL, Cattamanchi A, et al. Executive Summary: Official American Thoracic Society/ Centers for Disease Control and Prevention/ Infectious Diseases Society of America Clinical Practice Guidelines: Treatment of Drug-Susceptible Tuberculosis. *Clin Infect Dis.* 2016;63(7):853–67.
4. Heemskerk AD, Bang ND, Mai NTH, Chau TTH, Phu NH, Loc PP, et al. Intensified Antituberculosis Therapy in Adults with Tuberculous Meningitis. *N Engl J Med.* 2016;374(2):124–34.
5. Dian S, Yunivita V, Ganiem AR, Pramaesya T, Chaidir L, Wahyudi K, et al. Double-blind, randomized, placebo-controlled phase II dose-finding study to evaluate high-dose rifampin for tuberculous meningitis. *Antimicrob Agents Chemother.* 2018;62(12):1–12.
6. Cresswell FV, Te Brake L, Atherton R, Ruslami R, Dooley KE, Aarnoutse R, et al. Intensified antibiotic treatment of tuberculous meningitis. *Expert Rev Clin Pharmacol.* 2019 Mar;12(3):267–88.
7. Donald PR. Chemotherapy for Tuberculous Meningitis. *N Engl J Med [Internet].* 2016;374(2):179–81. Available from: <https://doi.org/10.1056/NEJMe1511990>
8. Cox H, Mizrahi V. The Coming of Age of Drug-Susceptibility Testing for Tuberculosis. *N Engl J Med.* 2018;379(15):1474–5.
9. Gumbo T, Angulo-Barturen I, Ferrer-Bazaga S. Pharmacokinetic-Pharmacodynamic and Dose-Response Relationships of Antituberculosis Drugs: Recommendations and Standards for Industry and Academia. *J Infect Dis.* 2015;211(Suppl 3):S96–106.
10. Naidoo A, Chirehwa M, Ramsuran V, McIlleron H, Naidoo K, Yende-Zuma N, et al. Effects of genetic variability on rifampicin and isoniazid pharmacokinetics in South African patients with recurrent tuberculosis. *Pharmacogenomics.* 2019;20(4):224–40.
11. Vinnard C, Ravimohan S, Tamuhla N, Ivaturi V, Pasipanodya J, Srivastava S, et al. Isoniazid clearance is impaired among human immunodeficiency virus/tuberculosis patients with high levels of immune activation. *Br J Clin Pharmacol.* 2017;83(4):801–11.
12. Vinnard C, Ravimohan S, Tamuhla N, Pasipanodya J, Srivastava S, Modongo C, et al. Markers of gut dysfunction do not explain low rifampicin bioavailability in HIV-associated TB. *J Antimicrob Chemother.* 2017;72(7):2020–7.
13. Weiner M, Peloquin C, Burman W, Luo CC, Engle M, Prihoda TJ, et al. Effects of tuberculosis, race, and human gene SLCO1B1 polymorphisms on rifampin concentrations. *Antimicrob Agents Chemother.* 2010;54(10):4192–200.
14. Jayaram R, Gaonkar S, Kaur P, Suresh BL, Mahesh BN, Jayashree R, et al. Pharmacokinetics-pharmacodynamics of rifampin in an aerosol infection model of tuberculosis. *Antimicrob Agents Chemother.* 2003;47(7):2118–24.
15. Gumbo T, Pasipanodya JG, Nuermberger E, Romero K, Hanna D. Correlations between the hollow fiber model of tuberculosis and therapeutic events in tuberculosis patients: Learn and confirm. *Clin Infect Dis.* 2015;61(Suppl 1):S18–24.
16. Vinnard C, King L, Munsiff S, Crossa A, Iwata K, Pasipanodya J, et al. Long-term mortality of patients with tuberculous meningitis in New York city: A cohort study. *Clin Infect Dis.* 2017;64(4):401–7.
17. Vinnard C, Winston CA, Wileyto EP, Macgregor RR, Bisson GP. Isoniazid resistance and death in patients with tuberculous meningitis: retrospective cohort study. *BMJ.* 2010 Sep;341:c4451.
18. Woods GL, Brown-Elliott BA, Conville PS, Desmond EP, Hall GS, Lin G, et al. 2nd edition. Wayne (PA): Clinical and Laboratory Standards Institute; 2011 Mar. Report No.: M24-A2. [Internet]. Wayne (PA); 2011. Available from: <https://www.ncbi.nlm.nih.gov/books/NBK544374/>
19. Hanke N, Frechen S, Moj D, Britz H, Eissing T, Wendl T, et al. PBPK Models for CYP3A4 and P-gp DDI Prediction: A Modeling Network of Rifampicin, Itraconazole, Clarithromycin, Midazolam, Alfentanil, and Digoxin. *CPT Pharmacometrics Syst Pharmacol.* 2018;7(10):647–59.

20. Rodgers T, Rowland M. Physiologically based pharmacokinetic modelling 2: predicting the tissue distribution of acids, very weak bases, neutrals and zwitterions. *J Pharm Sci.* 2006 Jun;95(6):1238–57.
21. Cordes H, Thiel C, Aschmann HE, Baier V, Blank LM, Kuepfer L. A physiologically based pharmacokinetic model of isoniazid and its application in individualizing tuberculosis chemotherapy. *Antimicrob Agents Chemother.* 2016;60(10):6134–45.
22. Lippert J, Burghaus R, Edginton A, Frechen S, Karlsson M, Kovar A, et al. Open Systems Pharmacology Community—An Open Access, Open Source, Open Science Approach to Modeling and Simulation in Pharmaceutical Sciences. *CPT Pharmacometrics Syst Pharmacol.* 2019;8(12):878–82.
23. Cresswell F V., Meya DB, Kagimu E, Grint D, Te Brake L, Kasibante J, et al. High-Dose Oral and Intravenous Rifampicin for the Treatment of Tuberculous Meningitis in Predominantly Human Immunodeficiency Virus (HIV)-Positive Ugandan Adults: A Phase II Open-Label Randomized Controlled Trial. *Clin Infect Dis.* 2021;73(5):876–84.
24. Kaojarern S, Supmonchai K, Phuapradit P, Mokkhavea C, Krittiyanunt sarinee. Effect of steroids on CSF penetration of antituberculous drugs in tuberculous meningitis. *Clin Pharmacol Ther.* 1991;49(1):6–12.
25. Brown TS, Narechania A, Walker JR, Planet PJ, Bifani PJ, Kolokotronis SO, et al. Genomic epidemiology of Lineage 4 *Mycobacterium tuberculosis* subpopulations in New York city and New Jersey, 1999-2009. *BMC Genomics* [Internet]. 2016;17(1):1–11. Available from: <http://dx.doi.org/10.1186/s12864-016-3298-6>
26. Woods GL, Brown-Elliott BA, Conville PS, Desmond EP, Hall GS, Lin G, et al. Susceptibility Testing of *Mycobacteria*, *Nocardiae*, and Other Aerobic Actinomycetes. 2nd editio. Wayne (PA): Clinical and Laboratory Standards Institute; 2011.
27. Rajman I, Knapp L, Hanna I. Genetic Diversity in Drug Transporters: Impact in African Populations. *Clin Transl Sci.* 2020 Sep;13(5):848–60.
28. Gumbo T, Louie A, Liu W, Brown D, Ambrose PG, Bhavnani SM, et al. Isoniazid bactericidal activity and resistance emergence: Integrating pharmacodynamics and pharmacogenomics to predict efficacy in different ethnic populations. *Antimicrob Agents Chemother.* 2007;51(7):2329–36.
29. Boeree MJ, Diacon AH, Dawson R, Narunsky K, Du Bois J, Venter A, et al. A dose-ranging trial to optimize the dose of rifampin in the treatment of tuberculosis. *Am J Respir Crit Care Med.* 2015;191(9):1058–65.
30. Davis A, Meintjes G, Wilkinson RJ. Treatment of Tuberculous Meningitis and Its Complications in Adults. *Curr Treat Options Neurol.* 2018;20(3).
31. Nau R, Djukic M, Spreer A, Eiffert H. Bacterial meningitis: new therapeutic approaches. *Expert Rev Anti Infect Ther* [Internet]. 2013;11(10):1079–95. Available from: <https://doi.org/10.1586/14787210.2013.839381>
32. Ruslami R, Gafar F, Yunivita V, Parwati I, Ganiem AR, Aarnoutse RE, et al. Pharmacokinetics and safety/tolerability of isoniazid, rifampicin and pyrazinamide in children and adolescents treated for tuberculous meningitis. *Arch Dis Child.* 2021;70–7.
33. Svensson EM, Dian S, Te Brake L, Ganiem AR, Yunivita V, Van Laarhoven A, et al. Model-Based Meta-analysis of Rifampicin Exposure and Mortality in Indonesian Tuberculous Meningitis Trials. *Clin Infect Dis.* 2020;71(8):1817–23.
34. Ding J, Thuy Thuong Thuong N, Pham T Van, Heemskerk D, Pouplin T, Tran CTH, et al. Pharmacokinetics and Pharmacodynamics of Intensive Antituberculosis Treatment of Tuberculous Meningitis. *Clin Pharmacol Ther.* 2020;107(4):1023–33.
35. Velásquez GE, Brooks MB, Coit JM, Pertinez H, Vásquez DV, Garavito ES, et al. Efficacy and safety of high-dose rifampin in pulmonary tuberculosis a randomized controlled trial. *Am J Respir Crit Care Med.* 2018;198(5):657–66.
36. Gliddon HD, Frampton D, Munsamy V, Heaney J, Pataillot-Meakin T, Nastouli E, et al. A Rapid Drug Resistance Genotyping Workflow for *Mycobacterium tuberculosis*, Using Targeted Isothermal Amplification and Nanopore Sequencing. *Microbiol Spectr.* 2021;9(3):1–12.

37. van Crevel R, Avila-Pacheco J, Thuong NTT, Ganiem AR, Imran D, Hamers RL, et al. Improving host-directed therapy for tuberculous meningitis by linking clinical and multi-omics data. *Tuberculosis* [Internet]. 2021;128:102085. Available from: <https://www.sciencedirect.com/science/article/pii/S1472979221000354>
38. Donovan J, Phu NH, Thao LTP, Lan NH, Mai NTH, Trang NTM, et al. Adjunctive dexamethasone for the treatment of hiv-uninfected adults with tuberculous meningitis stratified by leukotriene a4 hydrolase genotype (LAST ACT): Study protocol for a randomised double blind placebo controlled non-inferiority trial [version 1; r. Wellcome Open Res. 2018;3:1–19.
39. Donald PR, Schaaf HS, Schoeman JF. Tuberculous meningitis and miliary tuberculosis: the Rich focus revisited. *J Infect.* 2005 Apr;50(3):193–5.
40. Rock RB, Olin M, Baker CA, Molitor TW, Peterson PK. Central nervous system tuberculosis: Pathogenesis and clinical aspects. *Clin Microbiol Rev.* 2008;21(2):243–61.
41. Singh AK, Malhotra HS, Garg RK, Jain A, Kumar N, Kohli N, et al. Paradoxical reaction in tuberculous meningitis: Presentation, predictors and impact on prognosis. *BMC Infect Dis* [Internet]. 2016;16(1):1–11. Available from: <http://dx.doi.org/10.1186/s12879-016-1625-9>
42. Thiel C, Schneckener S, Krauss M, Ghallab A, Hofmann U, Kanacher T, et al. A systematic evaluation of the use of physiologically based pharmacokinetic modeling for cross-species extrapolation. *J Pharm Sci.* 2015 Jan;104(1):191–206.
43. Thomas L, Miraj SS, Surulivelrajan M, Varma M, Sanju CSV, Rao M. Influence of single nucleotide polymorphisms on rifampin pharmacokinetics in tuberculosis patients. *Antibiotics.* 2020;9(6):1–15.
44. Sloan DJ, McCallum AD, Schipani A, Egan D, Mwandumba HC, Ward SA, et al. Genetic determinants of the pharmacokinetic variability of rifampin in Malawian adults with pulmonary tuberculosis. *Antimicrob Agents Chemother.* 2017;61(7):1–9.
45. Tishkoff SA, Reed FA, Friedlaender FR, Ehret C, Ranciaro A, Froment A, et al. The genetic structure and history of Africans and African Americans. *Science* (80-). 2009;324(5930):1035–44.
46. Sekaggya-Wiltshire C, Chirehwa M, Musaaazi J, Von Braun A, Buzibye A, Muller D, et al. Low antituberculosis drug concentrations in HIV-tuberculosis-coinfected adults with low body weight: Is it time to update dosing guidelines? *Antimicrob Agents Chemother.* 2019;63(6):1–11.
47. Wasserman S, Davis A, Stek C, Chirehwa M, Botha S, Daroowala R, et al. Plasma pharmacokinetics of high-dose oral versus intravenous rifampicin in patients with tuberculous meningitis: a randomized controlled trial. *Antimicrob Agents Chemother.* 2021;65(8).

Supplementary Materials

S3.1. Generic Structure and Relevant Mechanistic Details of the PBPK Models for Rifampin and Isoniazid. The whole-body PBPK models for isoniazid and rifampin contains the relevant organs that play key roles in pharmacokinetics of drugs¹. The organs are represented by their volume and connected with each other by arterial and venous blood flows. Each organ, including brain, is further divided into blood, interstitial, and intracellular compartments. Reproduced from Thiel et al., 2015 and Kuepfer et al., 2016 under Creative Commons Attribution^{2,3}. Additionally, the rifampin and isoniazid PBPK models included all major contributing factors affecting systemic and CNS exposures, including, protein binding, active diffusion, passive transport, and relevant distribution and metabolism networks^{4,5}.



S3.2. Selection of the SNP Variant for Inclusion in Rifampin PBPK Analysis. Prior work has identified association of SLCO1B1 c.463CC (rs11045819 wild type) or c.463CA (rs11045819 heterozygous) genotypes with serum concentrations of rifampin in TB patients⁶. In our study, all SNPs identified in SLCO1B1 recognized in were evaluated for each subject⁷. Here, we performed a linkage disequilibrium analysis to characterize the association between various SLCO1B1 SNPs observed in our study data. A total of 32/40 patients had at least one heterozygous SNP. Four patients had heterozygous rs11045819 which was previously associated with lower rifampin Cmax. We identified other SNPs that were possibly associated with rs11045819 via linkage disequilibrium analysis. Two patients who did not have heterozygous rs11045819 SNP, but one or more associated SNP also had lower rifampin Cmax values in our dataset. Additionally, two patients who had heterozygous rs4149080 had lower rifampin Cmax. Previously, Sloan et al., 2017 observed that rs4149032 to be possibly associated with lower rifampin exposure however, our study did not demonstrate similar finding⁸. Patients who had rs11045819 heterozygous SNP were flagged in our dataset as SLCO1B1 heterozygous for evaluation in the PBPK model.

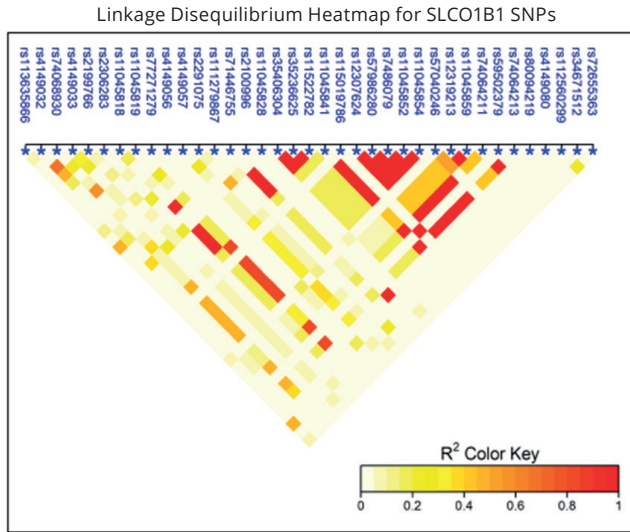
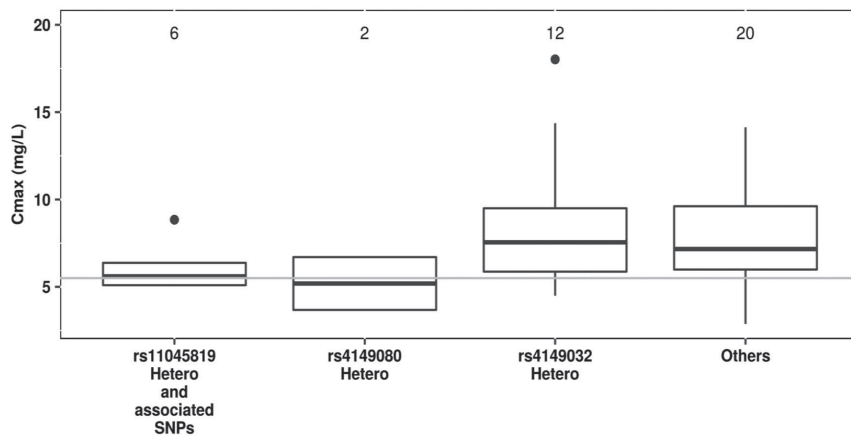


Table S3.3. List of SLCO1B1 SNPs associated with RS11045819

SLCO1B1 SNPs	rs11045819 (r ²)
rs11045841	0.82
rs11045852	0.82
rs11045854	0.82
rs12307624	0.82
rs57986280	0.82
rs74064211	0.82
rs74064213	0.82
rs74068930	0.57
rs7486079	0.82

S3.4. Observed C_{max} Stratified by SLCO1B1 SNP Groups



References

1. Lippert J, Burghaus R, Edginton A, Frechen S, Karlsson M, Kovar A, et al. Open Systems Pharmacology Community—An Open Access, Open Source, Open Science Approach to Modeling and Simulation in Pharmaceutical Sciences. *CPT Pharmacometrics Syst Pharmacol*. 2019;8(12):878–82.
2. Thiel C, Schneckener S, Krauss M, Ghallab A, Hofmann U, Kanacher T, et al. A systematic evaluation of the use of physiologically based pharmacokinetic modeling for cross-species extrapolation. *J Pharm Sci*. 2015 Jan;104(1):191–206.
3. Kuepfer L, Niederalt C, Wendl T, Schlender JF, Willmann S, Lippert J, et al. Applied Concepts in PBPK Modeling: How to Build a PBPK/PD Model. *CPT Pharmacometrics Syst Pharmacol*. 2016;5(10):516–31.
4. Hanke N, Frechen S, Moj D, Britz H, Eissing T, Wendl T, et al. PBPK Models for CYP3A4 and P-gp DDI Prediction: A Modeling Network of Rifampicin, Itraconazole, Clarithromycin, Midazolam, Alfentanil, and Digoxin. *CPT Pharmacometrics Syst Pharmacol*. 2018;7(10):647–59.
5. Cordes H, Thiel C, Aschmann HE, Baier V, Blank LM, Kuepfer L. A physiologically based pharmacokinetic model of isoniazid and its application in individualizing tuberculosis chemotherapy. *Antimicrob Agents Chemother*. 2016;60(10):6134–45.
6. Weiner M, Peloquin C, Burman W, Luo CC, Engle M, Prihoda TJ, et al. Effects of tuberculosis, race, and human gene SLCO1B1 polymorphisms on rifampin concentrations. *Antimicrob Agents Chemother*. 2010;54(10):4192–200.
7. Vinnard C, Ravimohan S, Tamuhla N, Pasipanodya J, Srivastava S, Modongo C, et al. Markers of gut dysfunction do not explain low rifampicin bioavailability in HIV-associated TB. *J Antimicrob Chemother*. 2017;72(7):2020–7.
8. Sloan DJ, McCallum AD, Schipani A, Egan D, Mwandumba HC, Ward SA, et al. Genetic determinants of the pharmacokinetic variability of rifampin in Malawian adults with pulmonary tuberculosis. *Antimicrob Agents Chemother*. 2017;61(7):1–9.

